



Original Article

Indirect effect of Covid-19 on Vegetation Indices around the cement plant of Gabes region

Ben Atia Zrouga Khaoula^{a,b,*}, Ben Amor Afef^c, Dridi Almohandes Bouthaina^d and Khebour Allouche Faiza^{a,b}

^aHorticultural Sciences and Landscape Department, Higher Agronomic Institute of Chott Mariem, University of Sousse, Sousse, Tunisia

^bLr GREE TEAM (LR17AGR01) INAT, University of Carthage, Tunis, Tunisia

^cDrylands and Oases Cropping Institute of Arid Regions of Mednine, University of Gabes, Mednine, Tunisia

^dUR13AGR08 "Environmental biochemistry and Eco-toxicology", Higher Agronomic Institute of Chott Mariem, University of Sousse, Sousse, Tunisia

ARTICLE INFO

Article history:

Received 25 January 2021

Revised 07 March 2021

Accepted 08 March 2021

Keywords:

Cement Plant;

Plant Cover;

Sentinel 2A;

Covid-19;

Radiometric Vegetation Indices.

ABSTRACT

To contain the Covid-19 pandemic, Tunisia imposed a national lockdown at the end of March 2020, a decision that resulted in a massive industrial complexes shutting down. The cement industry of Gabes was one of these complexes. However, to assess the impact of Covid-19 on the state of the vegetation around this industry three radiometric vegetation indices (RIs), NDVI, SAVI and EVI, were calculated from two Sentinel-2A imageries extracted at 22th December 2018 and 16th December 2020. Six plant species such as *Oleo europaea*, *Ficus caria*, *Medicago sativa*, *Prunus persica vulgaris*, *Zygophyllumalbum* and *Helianthemum kahiricum* were collected from 30 sites. Results suggest that, the period of pre-outbreak has the lowest averages of RIs. While, the after outbreak date has the higher levels of RIs presenting especially perennial species such as *Oleo europaea*. Then, EVI was the most higher index comparing to the rest of indices whatever the year studied. It was the most sensitive to cement dust and more susceptible to detect defoliation. Finally, through a remote application (RIs), the period of confinement allowed to improve the state of the vegetation surrounding the cement plant. It has helped the ecosystem to regenerate, especially perennial plant species.

1. Introduction

At the end of 2019, the appearance of the new coronavirus (SARS-CoV 2) in Wuhan, China has generated a global pandemic affecting the most countries in the world such as Africa, Europe, Asia and America [1,2]. The coronavirus affected 4.3 million people until May 2020 and caused 130.000 deaths [3]. To limit the spread of the virus, various social policies were adopted, which significantly affect the society and the economy. In fact, many activities including industry, tourism and travel have been stopped. As a result, air pollution, one of most challenging problem in the world, has significantly decreased. NO₂ concentrations are decreasing in Chinese cities as well as in several American and European countries [4, 5, 6, 7] with reduction of 20 and 30 % in China, Spain, Italy and France [6, 8, 9].

It was also determined that the tropospheric ozone was reduced in many countries according to Ozone Monitoring Instrument (OMI) and Board the Aura Satellite (NASA) [10].

In addition to gaseous pollutants, Particulate matter (PM), especially PM_{2.5} emitted by industrial activities has also reduced. Recent studies done by [11] showed that PM_{2.5} decreased up to 80 % during the lockdown period in many cities such Kuala Lumpur and Bangkok. In urban area, after imposing the restrictive measures, the use of vehicles was declined which participate in the reduce of both gaseous and particulate [12, 13].

Tunisia, as many other countries in the world, was affected by the corona virus in Mars 2020 causing around

* Corresponding author. Tel.: 0021650690652

E-mail address: kbenattia2017@gmail.com

Peer review under responsibility of University of Echahid Hamma Lakhdar.

2716-9227/© 2021 The Authors. Published by University of Echahid Hamma Lakhdar.. This is an open access article under the CC BY-NC license

(<https://creativecommons.org/licenses/by-nc/4.0/>).

<http://dx.doi.org/10.5281/zenodo.4592373>

119151 cases and 4126 deaths to date [3]. Under this situation, the governorate imposes control policies to limit the spread of the virus [14]. It shut down the national borders, stopped non-essential activities, closed restaurants and cafés, and, only 15 percent of employees were allowed to work in some companies.

These exceptional policies had an efficient effect to limit the spread of virus [15]. However, it has a significant negative impact on agriculture, tourism and in particular industry [16] which is considered as the most affected sector by Covid-19.

Gabes, one of the biggest industrial area in the south east of Tunisia, was characterized by various air pollutants such as hydrogen fluorides (HF), sulfur dioxide (SO₂) and Particulate Matter (PM) including heavy metals such as Zinc (Zn), Copper (Cu) and Lead (Pb) [17]. Tree-crop growing around industrial area can accumulate significant quantities of fluoride, around 150 µg/g DW in *Punica granatum* leaves [18] and 96 µg/g DW in leaf *Phoenix dactylifera* [19]. In fact, various biochemical and physiological process such as MDA content [19], chlorophyll content [20], relative water and ascorbic acid content air [21].

The cement industry of Gabes, one of major source of air pollution in Gabes region, affect the soil and the vegetation surrounding.

Because of Covid-19, around 81% of its activities has been stopped [22].

As a results, we suppose that stop can improve the health statue of vegetation and has positive impact in the environment.

Thus,-the objective of the present study is (i) to study the variation of three vegetation indices including NDVI (Normalized Vegetation Index), SAVI (Soil Adjusted Vegetation Index) and EVI (Enhanced Vegetation Index) and (ii) to assess the Covid-19 impact on the vegetation state using remote sensing.

2. Materials and Methods

2.1. Study area

The study was carried in the Gulf of Gabes (33° 88 '23' ' N, 10° 09' 90 'E), situated in the southeast of Tunisia, extending 700 km from the coast of the Mediterranean Sea, north to north from

Ras Kaboudia, and the Tunisian Libyan frontier in the south Fig.1.

This region covers an area of approximately 7166 km², has an arid climate with a mean annual precipitation between 167 and 176 mm, an average annual temperature between 18.8 and 19.3 C, and strong easterly winds impacting it [17]

Situated at 33°52' 20.31"N and 9°59' 25.56" E of Tunisia, the cement plant is one of the Tunisia's largest cement producer [23].

Based on the work of [17], 30 sites were selected containing six plant species such as two steppic vegetation (*Zygophyllum album* and *Helianthemum kahiricum*), three perennial species (*Oleo europaea*, *Ficus carica* and *Prunus persica vulgaris*) and one forage species which is presented by *Medicago sativa* to evaluate their vegetation indices before and since Covid-19.

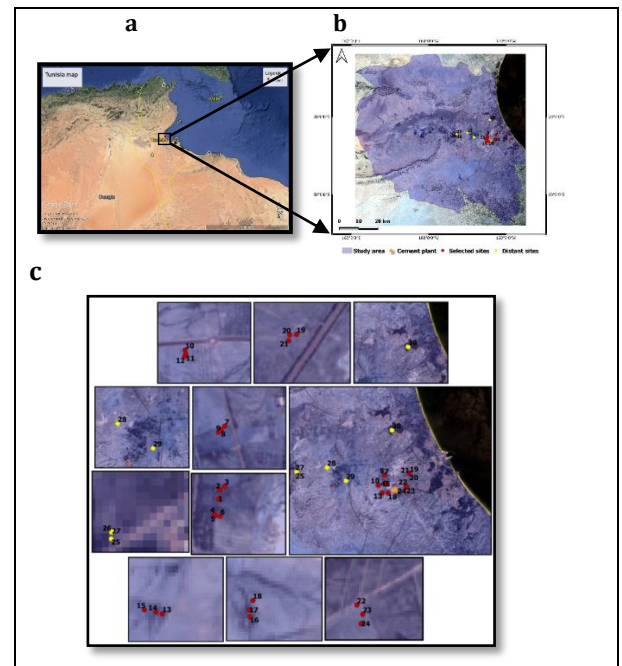


Fig 1. (a) Study area localization in Gabes-Tunisia; (b) cement factory and samples location; (c) zoom of selected and distant site samples.

2.2. Data collection

Based on the work of [17] which evaluate the plant contamination around the Gabes cement industry, 30 leaf sites were selected near and far away the cement factory.

The sites from 1 to 24 presented the sites located near the factory, and the rest (sites 25, 26, 27, 28, 29 and 30) presented samples distant from the cement plant.

Six plant species: *Oleo europaea*, *Ficus carica*, *Prunus persica vulgaris*, *Medicago sativa*, *Zygophyllum album* and *Helianthemum kahiricum* are the predominant species in the different studies sites.

The sampling sites and plants occupation are presenting in Table 1.

Table 1. Plant species and sites localization number.

Plant species	Site localization number	
	Selected	Distant
<i>Oleo europaea</i>	1, 2, 3, 7, 8, 9, 23, 24	25, 30
<i>Ficus carica</i>	13, 14, 15, 22	-
<i>Prunus persica vulgaris</i>	-	26
<i>Medicago sativa</i>	-	27
<i>Zygophyllum album</i>	4, 5, 6, 16, 17, 18	29
<i>Helianthemum kahiricum</i>	10, 11, 12, 19, 20, 21	28

2.3. Downloading of satellite images

Two Sentinel 2-A satellite images have been downloaded for free from ESA site [13]. The satellite images present two different dates: the first date was 22th December 2018, before the Covid-19, corresponding to the field companies in 2018; the second was registered at 16th December 2020 since Covid-19 corresponding to the confinement period whose field access was impossible. For that reason, the choice of this image in the same period of the first companies was necessary.

In 2018, precipitation decreased gradually from October (24.2 mm), November (17.9 mm) to December (1.6 mm). While PM10 increased from October (0.05 mg/m³) to December (0.07 mg/m³) referring to the air quality data of the study area [24]. The dominant wind directions were from the south and west-southwest in these three consecutive months. In 2020, rainfall increased from October (9.14 mm) to November (27.42 mm) and decreased in December (17 mm) following the same wind directions as 2018. PM10 in this period was not available.

Table 2. Satellite images characteristics.

	Identifier	Acquisition date	Instrument
Image 1	S2A_MSIL1C_2	22/12/2018	MSI
	0181222T100421		
	_N0207_R122_T		
	32SNC_2018122		
	2T103540		
Image 2	S2B_MSIL1C_2	26/12/2020	MSI
	0201216T100329		
	_N0209_R122_T		
	32SNC_2020121		
	6T105857		

2.4. Preprocessing of Satellite Images

This processing consists in making an atmospheric

correction to each one of the satellite images chosen using the QGIS 3.8.3 software which allows these 2 downloaded images to be preprocessed in a very short time.

The method proposed in this work is called "Dark Object Subtraction" (DOS: dark object subtraction model), which does not require any user intervention. Only a good knowledge of the processing scene content with a library spectral containing all materials signatures in this same scene are sufficient.

2.5. Processing of satellite images

For the Sentinel 2 satellite, the red, near infrared and blue spectral bands are represented by channels B4, B8 and B2 respectively.

Using QGIS 3.8.3, the three radiometric vegetation indices (Table.3) were calculated by entering the band math and the formula of each satellite image in this software. Then, for each site the pixel value of NDVI, SAVI and EVI was taken. Finally, the data processed by QGIS 3.8.3 is transferred to Excel in order to draw indices curves.

Table 3. Vegetation indices used.

Indices	Equation	Reference
Normalized Difference Vegetation index (NDVI)	$(PIR - R) / (PIR + R)$	[25]
Enhanced Vegetation Index (EVI)	$2.5 * [(NIR - RED) / ((NIR) + (6RED) - (7.5BLUE) + 1)]$	[26]
Soil-Adjusted Vegetation Index (SAVI)	$[(NIR - Red) / (NIR + Red + L)] * (I + L)$ Avec $L = 0.5$	[27]

3. Results and Discussion

3.1. Temporal and Spatial Distribution of Radiometric Vegetation Indices (RIs)

The RIs includes NDVI, SAVI and EVI from 30 sites during 2018 and 2020 was presented in Fig.2

The maximum values of NDVI, SAVI and EVI were 0.45, 0.28 and 0.45 respectively in 2018. While in 2020 were corresponding to 0.56, 0.30 and 0.43. This variation may be related in part to the meteorological conditions recorded in 2020 specially on the date of image acquisition as it is qualified as rainy (17 mm in December) compared to December of 2018 (1.6 mm). Also confinement can attribute to reduce cement dust essentially (higher RIs in 2020) since the industry was closed.

Regardless weather conditions, spatial analysis of

radiometric vegetation indices suggest an increasing behavior moving away from the cement plant for the two selected dates. Their values are always low around the cement plant, and higher far away from this last. The sites (from 1 to 24), located near to the factory, presented a low to medium values of NDVI, SAVI and EVI varied from 0.06 to 0.12 in 2018. Higher contents of these indices qualified specially *Oleo europaea*, *Ficus carica* and *Helianthemum kahiricum* occupying specially sites 7, 8, 13, 19, 20, 21, 22, 23 and 24 for NDVI (0.13, 0.10, 0.10, 0.11, 0.11, 0.10, 0.09, 0.11 and 0.12 respectively) and sites 19 to 24 for SAVI (0.09 to 0.10). For EVI, the higher contents are noted in sites 4 (0.09), 7 (0.09, 8 (0.09), 13 (0.09), 16 (0.09), 17 (0.10), and varied from 0.11 to 0.12 from sites 19 to 24. While a very higher contents of these indices were noted in distant sites. Only, sites 26 and 27 have a lower values compared to the other distant sites. They are occupied by *Prunus persica vulgaris* and *Medicago sativa* qualifying the control oasis land. Their values were 0.09, 0.07 and 0.09 respectively for NDVI, SAVI and EVI for site 26 and 0.10, 0.09 and 0.10 respectively for site 27. The higher levels of these indices (0.45, 0.28 and 0.45 respectively) marked specially *Oleo europaea* (site 30).

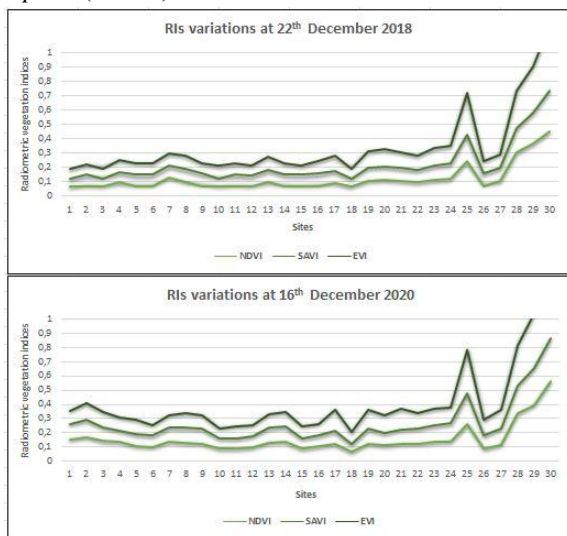


Fig 2. RIs variations in 2018 and 2020 extracted from 30 sites.

In 2020, the same behavior was noted. The selected sites presented the lower contents of RIs compared to the distant sites from the cement industry. Higher values of NDVI are related to sites 1 and 2 which were occupied by *Oleo europaea* and varied from 0.15 to 0.17 respectively. Sites 1, 2, 13, 22, 23 and 24 have the larger levels of SAVI (0.11 to 0.12). For EVI, sites 2, 3, 8, 19, 20, 21, 22, 23 and 24 have the most higher values of this index and varied respectively from 0.12, 0.11, 0.11, 0.13, 0.13, 0.14, 0.11, 0.12 and 0.12.

Sites 25, 28, 29 and 30, located far to the factory, have the higher values of all RIs characterizing steppic vegetation and *Oleo europaea*. Site 30 has the highest NDVI (0.56) compared to EVI and SAVI.

For the two date periods, NDVI was the most lower while EVI was the most higher. Site 25 and 30 occupying by *Oleo europaea* species presented the larger peaks of the three RIs comparing to the other sites.

3.2. Spatial distribution mapping of RIs around the cement plant

The multi-date mapping of the NDVI, SAVI and EVI is given in Fig.3. It should be remembered in this context that lower values of RIs reflect the absence of vegetation or dry vegetation whereas higher values indicate a more dominant presence and photo-synthetically active vegetation. In these figures, the colors red, green and blue represent an increasing RIs values and therefore better plant cover.

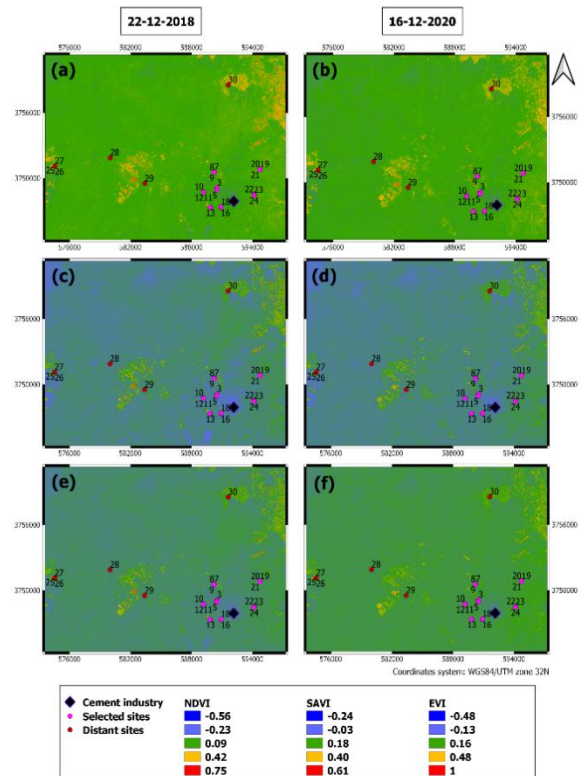


Fig 3. Spatial distribution mapping of RIs: (a) NDVI 2018; (b) NDVI 2020; (c) SAVI 2018; (d) SAVI 2020; (e) EVI 2018 and (f) EVI 2020 around cement plant.

At a local scale, NDVI mapping shows the same behavior comparing to the two dates with intervals varied from -0.56 to 0.75. While SAVI and EVI present similar maps to have an intervals compromised between -0.24 to 0.61 for SAVI and -0.48 and 1 for EVI reflecting lower values near the cement industry (selected sites) and higher

contents in the distant sites which can be due to the higher deposition of cement dust near the factory. However, the date selected in 2020 has the highest levels of the three indices relating to the higher precipitation recorded in the month of the image acquisition.

A general examination of all results shows a spatiotemporal variation of the vegetation radiometric indices in relation to the environment physical, bioclimatic and anthropogenic components. Indeed, temporal analysis of NDVI, SAVI and EVI showed a trend towards low values in 2018.

This is probably related to the meteorological and agro-pedological factors of the environment which are decisive in the growth cycle of plants and therefore of the variation in the intensity of chlorophyll activity measured by these indices, or at the rate and distribution of rains during these years [28]. So a drier year which is the case of 2018 had an effect on the plants' spectral response [29] by changing vegetation greenness [30].

It is noted that the vegetation systematically turns green with each increase in chlorophyll activity with rains and a strong wetting power of the soil. Higher indices values indicate a larger fraction of vegetation in a pixel [31].

This is the case of 2020 (17 mm in December) which shows a strong trend towards high values of all RIs associated generally to greener species such as *Oleo europaea*.

The high content of these indices during 2020 may be explained also by the low degradation caused by the cement plant for the plant cover since air pollution degree (PM₁₀, SO₂, NO₂, etc.) decreased in the lockdown period of Covid-19, having so a direct repercussion on environment and vegetation crops [32].

Some reports have shown that the Covid-19 outbreak lowered air pollution largely due to the decline in transport and financial activities [8, 33, 34]. More precisely, [9] found a 30% reduction in air pollution in populated cities such as Wuhan, Italy, Spain USA, etc.

Another study conducted in Tehran, Iran, shows that despite having more rainfall compared to the same time last year, the pandemic has led to higher outdoor particulate matter air pollution due to the use of more personal transport [35].

Spatially, and moving away from cement plant, an increase in the mean values of the NDVI, SAVI and EVI was noted. In fact, the lower values of these indices were noted near the cement plant (selected sites) while the higher values were observed in the distant sites. This indicates that close to this industry, the vegetation cover is

more degraded than that located far away. This is probably due to the deposition effect of various dust. Which means that, moving further away from this factory, dust deposition will be decreased. This result confirms that of [36] who found a tendency for the chlorophyll content of plants to increase in association with the decrease in the deposition of cement dust at increasing distance from the plant.

EVI was the radiometric vegetation index the most sensitive to cement dust by inducing different spectral response from 2018 to 2020. [37] showed that in high biomass conditions and atmospheric effect on the spectral signal, EVI is more resistant to reflectance saturation compared to NDVI.

Our study area is relatively polluted, high cement emissions may have led to EVI being more susceptible to defoliation than NDVI and SAVI.

4. Conclusion

In recent months' and related to human health, the spread of the Covid-19 pandemics worldwide was worrying. On the other hand, this is proven to be advantageous for the environment by reduction air emissions which has a large repercussion especially for vegetation crops. In Tunisia, the after outbreak of this pandemic caused a higher level of spectral signature of vegetation qualifying by higher values of three radiometric indices NDVI, SAVI and EVI of some plant species selected in this work especially for *Oleo europaea*. The over contents of these indices was

associated basically with a larger level of precipitation presenting essentially 2020, period of after lockdown Covid-19. Then, control leaf sites have the most higher averages of the three radiometric vegetation indices due to cement deposition in both of years studied. Thus, it is necessary to focus on the critical points of cement air pollution, and work on them not only at a distant scale, but also in-situ.

Acknowledgements

The present research has been financially supported by the Tunisian Ministry of High Education and Scientific Research, which provided a PhD scholarship for the student Zrouga Ben Atia Khaoula.

Conflict of Interest

The authors declare that they have no conflict of interest.

References

1. Chen K, Wang M, Huang C, Kinney P L & Anastas P T. Air pollution reduction and mortality benefit during the COVID-19 outbreak in China. *The Lancet Planetary Health*. 2020, 4;6 : 210-212.
2. Huang C, Wang Y, Li X, Ren L, Zhao J, Hu Y & Cao B. Clinical features of patients infected with 2019 novel

- coronavirus in Wuhan, China. *The Lancet*. 2020, 395;10223: 497–506. [https://doi.org/10.1016/S0140-6736\(20\)30183-5](https://doi.org/10.1016/S0140-6736(20)30183-5)
3. WHO World Health Organization. Coronavirus disease (COVID-19) Weekly epidemiological and Operational updates December. 2020.
 4. Shrestha A M, Shrestha U B, Sharma R, Bhattarai S, Tran H N T & Rupakheti M. No Lockdown caused by COVID -19 pandemic reduces air pollution in cities worldwide Title. *Environ Poll*. 2020. <https://doi.org/10.31223/osf.io/edt4j>
 5. Tobías A, Carnerero C, Reche C, Massagué J, Via M, Minguillón M C, Alastuey A & Querol X. Changes in air quality during the lockdown in Barcelona (Spain) one month into the SARS -CoV -2 epidemic. *Sci Total Environ*. 2020. 726: 138540. <https://doi.org/10.1016/j.scitotenv.2020.138540>
 6. Wang, Q., Su, M. A preliminary assessment of the impact of COVID -19 on environment—A case study of China. *Sci Total Environ*. 2020, 728: 138915. <https://doi.org/10.1016/j.scitotenv.2020.138915>
 7. Zhang R, Zhang Y, Lin H, Feng X, Fu T M & Wang Y. NOx Emission Reduction and Recovery during COVID -19 in East China. *Atmosphere*. 2020, 11: 4. <https://doi.org/10.3390/atmos11040433>
 8. Dutheil, Frédéric, Baker J S & Navel V. COVID-19 as a factor influencing air pollution? *Environmental Pollution*. 2020, 263: 2019-2021. <https://dx.doi.org/10.1016%2Fj.envpol.2020.114466>
 9. Muhammad S, Long X & Salman M. COVID -19 pandemic and environmental pollution: A blessing in disguise?. *Sci Total Environ*.2020, 138820. <https://doi.org/10.1016/j.scitotenv.2020.138820>
 10. Kanniah, K. D., Kamarul Zaman, N. A. F., Kaskaoutis, D. G., & Latif, M. T. (2020). COVID-19's impact on the atmospheric environment in the Southeast Asia region. *Science of the Total Environment*, 736, 139658. <https://doi.org/10.1016/j.scitotenv.2020.139658>
 11. Arkin F. Pollutants, Asian COVID-19 lockdowns clear the air of pollutants. *Sci Dev Net* ,(https://www.scidev.net/asia-pacific/news/asian-covid-19-lockdowns-clear-the-air-of-pollutants/),2020.
 12. CAMS. Atmosphere copernicus amid coronavirus outbreak copernicus monitors reduction particulate matter PM2.5 over china.2020.
 13. ESA European Space Agency. (2020)
 14. Tunisian Republic Presidency.2020.
 15. BenMiled S & Kebir A. Simulations of the spread of COVID-19 and control policies in Tunisia, ArXiv, 2020:1–11.<https://arxiv.org/pdf/2005.00750.pdf>
 16. Elkadhi Z, Elsbabgh D, Frija A, Lakoud T, Wiebelt M & Breisinger C. The impact of Covid-19 on Tunisia's economy, Agri-food System, and Households. Middle East and North Africa IFPRI. 2020; 13.
 17. Ben Atia Zrouga K, Mendes M P, Falcão A P, Almohandes B D, Hachicha M & Khebour Allouche F. Mapping heavy metal (Cu, Zn, and Pb) pollution and ecological risk assessment, in the surroundings of Gabes cement plant - Tunisia. *International Journal of Phytoremediation*. 2020: 1-8. <https://doi.org/10.1080/15226514.2020.1869177>
 18. Elloumi N, Ben Amor A, Zouari M, Belhaj D, Ben Abdallah F & Kallel M. Adaptive biochemical responses of Punica Granatum to atmospheric fluoride pollution. *Fluoride*. 2016, (49) 3 : 357–365.
 19. Ben Amor A, Elloumi N, Chaira N & Nagaz K. Morphological and Physiological Changes Induced in the Date Palm Trees (Phoenix dactylifera) Exposed to Atmospheric Fluoride Pollution.*Tunisian Journal of Plant Protection*. 2018, 13;1:11-22.<http://www.tjpp.tn/SiteWeb/TJPPsi2018/CurrentIssue/TJPPsi2018.pdf>
 20. Nadgórska-Socha A, Kandziora-Ciupa M, Trzęsicki M & Barczyk G. Air pollution tolerance index and heavy metal bioaccumulation in selected plant species from urban biotopes. *Chemosphere*. 2017, 183 : 471 _482. <https://doi.org/10.1016/j.chemosphere.2017.05.128>
 21. Ben Amor A, Bagues Mohamed, Elloumi N, Chaira N, Rahmeni Rami & Nagaz K. Suitability of four main Mediterranean tree crop for their growth in peri- urban agriculture and restoration (Gabes, Tunisia). *Environ Sci Pollut Res*. 2021.<https://doi.org/10.1007/s11356-020-12102-2>
 22. Mansour N & Salem S Ben. Socio-Economic Impacts of Covid-19 on the Tunisian Economy. *Journal of the International Academy for Case Studies*. 2020, 26(4): 1–13.
 23. Haydar A. Industrialisation de gabes et ses conséquences : Etude géographie urbaine et économique. Université de Tunis ; 1987 : 332.
 24. ANPE. National Agency of Environmental Protection of Tunisia.2018.
 25. Rouse J W, Haas R H, Schell J A, Deering DW & Harlan J C. Monitoring the Vernal Advancement and Retrogradation of Natural Vegetation. In NASA/GSFC, Greenbelt, MD; 1974: 371.
 26. Huete A R, Liu H Q, Batchily K & Van W L. A comparison of vegetation indices global set of TM images for EOS-MODIS. *Remote Sensing of Environment*. 1997, 59 ; 3 :440–451. [https://doi.org/10.1016/S0034-4257\(96\)00112-5](https://doi.org/10.1016/S0034-4257(96)00112-5)
 27. Huete A R. A soil-adjusted vegetation index (SAVI). *Remote Sensing of Environment*. 1988, 25: 295–309. [https://doi.org/10.1016/0034-4257\(88\)90106-X](https://doi.org/10.1016/0034-4257(88)90106-X)
 28. Diello P, Mahe G, Paturel J E, Dezetter A, Delclaux F, Servat E & Ouattara F. Relationship between Rainfall and Vegetation Indexes in Burkina Faso: A Case Study of the Nakambé Basin. *Hydrological Sciences Journal*. 2005, 50;2.<https://doi.org/10.1623/hysj.50.2.207.61797>
 29. Walker J J, de Beurs K M & Wynne R H. Dryland vegetation phenology across an elevation gradient in Arizona, USA, investigated with fused MODIS and Landsat data. *Remote Sensing of Environment*. 2014, 144: 85–97. <https://doi.org/10.1016/j.rse.2014.01.007>
 30. Zhou J, Jia L, Menenti M, van Hoek M, Lu J, Zheng C & Yuan X. Characterizing vegetation response to rainfall at multiple temporal scales in the Sahel-Sudano-Guinean region using transfer function analysis. *Remote Sensing of Environment*. 2021, 252; 20 : 112108. <https://doi.org/10.1016/j.rse.2020.112108>
 31. Firozjaei M K, Kiavarz M, Alavipanah S K, Lakes T & Qureshi S. Monitoring and forecasting heat island intensity through multi-temporal image analysis and cellular automata-Markov chain modelling: A case of Babol city, Iran. *Ecological Indicators*. 2018, 91: 155-170. <https://doi.org/10.1016/j.ecolind.2018.03.052>
 32. Ju M J, Oh J & Choi Y H. Changes in air pollution levels after COVID-19 outbreak in Korea. *Science of the Total Environment*. 2021, 750:

141521. <https://doi.org/10.1016/j.scitotenv.2020.141521>
33. Afshari R. Indoor air quality and severity of Covid- 19 Where communicable and non- communicable preventive measures meet. Archives of Bone and Joint Surgery. 2020, 9;1:1-2. <https://dx.doi.org/10.22038/apjmt.2020.15312>
 34. Asna-asharya M, Farzaneganb, Mohammad Reza Malek, Mehdi Feizia, Saeed & Sadati. COVID-19 Outbreak and Air Pollution in Iran: A Panel VAR Analysis. No. 16-2020, Philipps-University Marburg, Joint Discussion Paper Series in Economics, School of Business and Economics, Marburg. 2020. <http://hdl.handle.net/10419/216656>
 35. Faridi S, Yousefian F, Niazi S, Ghalhari M R, Hassanvand M S & Naddafi K. Impact of SARS-CoV-2 on ambient air particulate matter in Tehran. Aerosol and Air Quality Research. 2020, 20(8): 1805–1811.
 36. Odu EA. Impact of cement dust emission on leaf chlorophyll of agricultural crops. Proceeding on environmental monitoring and impact assessment seminar (EEC). 1994: 404- 410
 37. Huete A, Didan K, Miura T, Rodriguez E P, Gao X, Ferreira L G. Overview of the radiometric and biophysical performance of the MODIS vegetation indices. *Remote Sensing of Environment*. 2002, 83, 1;2: 195 – 213

Recommended Citation

Ben Atia Zrouga K, Ben Amor A, Dridi Almohandes B and Khebour Allouche F. Indirect effect of Covid-19 on Vegetation Indices around the cement plant of Gabes region. *Alg. J. Eng. Tech.* 2021, 4:59-65. <http://dx.doi.org/10.5281/zenodo.4592373>



This work is licensed under a [Creative Commons Attribution-NonCommercial 4.0 International License](https://creativecommons.org/licenses/by-nc/4.0/)